BIOMICROFLUIDICS **9**, 054111 (2015)

Flip channel: A microfluidic device for uniform-sized embryoid body formation and differentiation

Ying-Hua Chen, Chien-Chung Peng, and Yi-Chung Tung[a)]
Research Center for Applied Sciences, Academia Sinica, Taipei 11529, Taiwan

(Received 20 May 2015; accepted 11 September 2015; published online 29 September 2015)

This paper reports a two-layered polydimethylsiloxane microfluidic device—Flip channel, capable of forming uniform-sized embryoid bodies (EBs) and performing stem cell differentiation within the same device after flipping the microfluidic channel. The size of EBs can be well controlled by designing the device geometries, and EBs with multiple sizes can be formed within a single device to study EB size-dependent stem cell differentiation. During operation of the device, cells are positioned in the designed positions. As a result, observation and monitoring specific population of cells can be achieved for further analysis. In addition, after flipping the microfluidic channel, stem cell differentiation from the EBs can be performed on an unconfined flat surface that is desired for various differentiation processes. In the experiments, murine embryonic stem cells (ES-D3) are cultured and formed EBs inside the developed device. The size of EBs is well controlled inside the device, and the neural differentiation is performed on the formed EBs after flipping the channel. The EB size-dependent stem cell differentiation is studied using the device to demonstrate its functions. The device provides a useful tool to study stem cell differentiation without complicated device fabrication and tedious cell handling under better-controlled microenvironments.
© *2015 AIP Publishing LLC*. [http://dx.doi.org/10.1063/1.4931638]

I. INTRODUCTION

Embryonic stem (ES) cells have been widely discussed for their pluripotency and self-renewability. ES cells can differentiate to various kinds of cells, such as cardiomyocytes, hematopoietic progenitors, and dopaminergic neurons.[1] For a better recapitulation of ES cell differentiation, the formation of an embryoid body (EB) is pivotal.[2,3] It is well known that microenvironmental factors have a profound impact on directing the differentiation fate of EBs. One of the most important factors is the size and morphology of EBs.[1,4–7] For example, Hwang *et al*.[8] demonstrated that cardiogenesis was enhanced in larger EBs, while endothelial cell differentiation was increased in smaller EBs. Furthermore, Choi *et al*.[9] performed stem cell differentiation from the EBs with controlled dimensions, and they found that the cardiogenesis and neurogenesis were strongly regulated by the EB dimensions. Although many conventional methods have been reported to produce uniform-sized spheroids, such as hanging drop, spinner flask, and round-bottomed 96-well plate cultures, it still requires a lot of effort for forming homogenous and uniform-sized EBs, and it is usually tedious to transfer EBs for the following differentiation processes.[2] Furthermore, recent studies have found the stem cells begin to self-organize themselves in EBs and further affect their latter differentiation.[10,11] Therefore, a technique allowing researchers monitor and image specific EBs from their formation to differentiation is highly desired for stem cell research.

Because of the automation capability and better spatiotemporal controllability provided by microfluidic techniques, various microfluidic cell culture devices have been developed to better study cells under physiological meaningful microenvironments *in vitro*.[12–20] Moreover, a microfluidic device capable of precisely positioning EBs to study their differentiation under various controlled

[a)]Author to whom correspondence should be addressed. Electronic mail: tungy@gate.sinica.edu.tw. Tel.: +886-2-2787-3138; Fax: +886-2-2787-3122.

 © 2015 AIP Publishing LLC

microenvironment factors, including chemical and physical ones, is highly desired for stem cell researches.[21,22] As a result, a variety of microfluidic devices are proposed to simplify the EB formation and differentiation processes.[3,23–27] These microfluidic devices provide efficient tools for massive uniform-sized EBs production; however, it is difficult and tedious to harvest and transport the EBs for subsequent differentiation studies in unconfined spaces comparable to those done in Petri dishes. In addition, continuous monitoring of each EB and study differentiation of the EBs with different sizes are also challenging in the current setups. For instance, the microfluidic devices with sandwiched semi-porous membranes can easily produce EBs with homogeneous dimensions controlled by the geometry design of the channels. However, the non-optically transparent semi-porous membrane and relative long distance between samples and objectives limit the optical imaging capability on EBs.[3] The differentiation can also be performed within the same device; however, the cells are cultured in the compartmentalized channel with spatial confinement.[3] Several concave microwell devices have been also developed for EB formation and differentiation studies. In these devices, the EBs need to be manually transferred to Petri dishes after the formation, which makes continuous observation of specific EBs challenging. For example, Choi *et al.*[9] formed uniform-sized EBs using concave microwell structures and retrieved them onto tissue culture dishes for neuronal differentiation studies. Recently, Kang *et al.*[23] reported a microfluidic device capable of forming uniform-sized EBs and performed cell differentiation within the same device. However, each time only single-sized EB can be formed in the device with careful control of the flow rates. In addition, the device structures confine the spaces (with lateral dimension of approximate 500 μm) for stem cell differentiation, which may limit the differentiated cell expansion (often needs lateral dimension of mm) and introduce additional undesired physical factors for the cells.

This paper reports a simple microfluidic device—Flip channel, which is capable of efficiently forming uniform-sized spheroids, and the size of EBs can be controlled by geometry design of the microfluidic channel in a straightforward manner.[26] Moreover, by flipping over the device, the EBs are able to attach to the desired positions within the microfluidic channel. The device allows the proceeding stem cell differentiation studies without sophisticated sample handling, transportation, and spatial confinement in well structures, and the device also enables continuous observation and imaging on specific EBs from their formation to differentiation. Furthermore, the conventional cell analysis and observation schemes utilized in biological laboratories can be directly applied for the further studies. In the experiments, murine embryonic stem (mES) cells are cultured to form EBs inside the developed device. The EB sizes are analysed to confirm the EB size controllability of the device. After the EB formation, the microfluidic channel is flipped over to perform stem cell differentiation. Specifically, neuronal differentiation is performed, and the EB size-dependent neurogenesis is studied in this paper. The experimental results demonstrate that the developed device provides a powerful tool for stem cell research, and the device can be operated in a simple manner. Moreover, the device can be integrated with other microenvironment control functions provided by microfluidics to advance the stem cell researches.

II. MATERIALS AND METHODS

A. Microfluidic device design and fabrication

The entire device is made of an elastomer material, polydimethylsiloxane (PDMS), due to its great optical transparency, gas permeability, manufacturability, and biocompatibility. The device is constructed of two PDMS layers: the channel layer and the chamber layer as shown in Fig. 1. In the channel layer, a straight microfluidic channel (width $\times$ length $\times$ height: 5 mm $\times$ 3 cm $\times$ 250 μm) with pillars (diameter: 50 μm) is designed for cell delivering and EB differentiation without spatial confinement. In the chamber layer, cubical aliquot chambers with various dimensions are exploited to aliquot ES cells. The rectangular chambers with flat surfaces can provide better imaging quality without distortion. Furthermore, the master molds to fabricate the chambers during the replica mold process can be fabricated using straightforward photolithography processes with great dimension control and consistency.

The entire microfluidic device is fabricated using the well-developed multi-layer soft lithography (MSL) replica molding technique. The microfluidic device is made of the

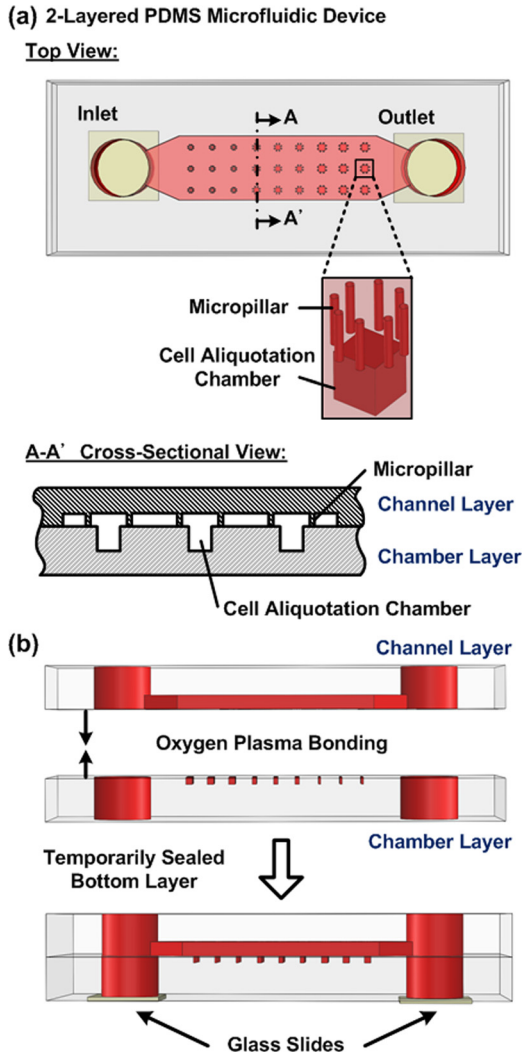

FIG. 1. (a) Schematic and cross-sectional view of the two-layered PDMS microfluidic devices for uniform-sized EB formation and differentiation. (b) Fabrication process of the flip channel microfluidic device.

commercially available elastomeric material, PDMS (Sylgard 184, Dow Corning, Midland, MI), cast against silicon wafer molds with SU-8 (SU-8 2100, MicroChem Corp., Westborough, MA) microfluidic channel features with thicknesses of approximately 250 μm patterned by conventional photolithography and then silanized by 1H,1H,2H,2H-perfluorooctyl trichlorosilane (91%) (L16606, Alfa Aesar, Ward Hill, MA) in a desiccator. The two PDMS layers are aligned and irreversibly bonded using an oxygen plasma surface treatment (90 W) for 40 s (PX-250, Nordson MARCH, Concord, CA).[28] The inlet and outlet (2 mm in diameter) are then punched after the bonding process. After the device fabrication, 5% (w/v) bovine serum albumin (BSA, A2058, Sigma-Aldrich, St. Louis, MO) in water is introduced into the microfluidic channel and incubated for 2 h to eliminate the cell-substrate interaction within the device. Prior to cell seeding, normal culture medium is exploited to wash out the excessive BSA.

B. ES cell culture

To demonstrate the device capability, mES cells (ES-D3, 60205, Bioresource Collection and Research Center, Hsinchu, Taiwan) transfected with Oct4-GFP (hOct4-GFP, Plasmid 21153, Addgene, Cambridge, MA) are utilized in the experiments. The ES-D3 cells are cultured using growth medium composed of Dulbecco's Modified Eagle Medium (DMEM) (Gibco 10566,

Invitrogen, Calrsbad, CA) with 15% v/v fetal bovine serum (FBS) (Gibco 10082, Invitrogen), 1% v/v antibiotic/antimycotic (Gibco 15240, Invitrogen), 0.1 mM 2-mercaptoethanol (M7522, Sigma-Aldrich), 0.02% v/v sodium pyruvate (Gibco 11360, Invitrogen), 1% v/v non-essential amino acid (Gibco 11140, Invitrogen), and 1000 U ml^{-1} ESGRO (Chemicon ESG1106, Millipore). The stocks are maintained in 1% gelatin (G1890, Sigma-Aldrich)-coated Petri dishes at 37 °C in a humidified incubator with 5% CO_2. The growth medium is changed one day after seeding, and the cells are sub-cultured every other day. The ES-D3 cells are passaged by dissociation with TrypLE Express (Gibco 12605, Invitrogen), and cell suspensions for the experiments are made by centrifugation of dissociated cells at 1000 rpm for 5 min at room temperature.

C. EB formation and differentiation

Figure 2 shows the ES cell seeding, EB formation, and differentiation processes. First, the ES-D3 cells with density of 2×10^7 cells/ml are introduced into the device through the channel layer using a gravity-driven flow. The cells settled down into the aliquot chambers within 15 min, and the culture medium is then introduced into the channel layer again using the gravity driven flow to remove the non-aliquot cells as shown in Fig. 2(a). After 15 min of static culture, both the inlet and outlet of the channel layer are temporally covered by glass slides, and the device is flipped upside down. All the loosely aggregated cells fall onto the channel layer within 30 min, and the EBs are formed due to the strong cell-cell interaction after 16 h of static culture (Fig. 2(b)). The medium is exchanged everyday using the gravity-driven flow, and the medium can be exchanged efficiently due to the straight flow channel design.[26]

To demonstrate that the EB differentiation can be achieved within the same device without additional sample transportation, neurogenesis of ES cells is performed in the experiment according to the protocol from a commercial kit (SCR101, Millipore, Billerica, MA). After flipping the channel, the flat and unconfined channel layer surface within the device makes the device an excellent tool for the neural development study of EBs. Because the immature neurons need to travel a long way from embryo to their final destination in neural development, space is an essential element not only for the outgrowth of axons and dendrites but also for the neuronal migration.

After the formation of EBs, they are cultured statically in the growth medium in the absence of leukemia inhibitory factor (LIF) for an additional three days (3− condition) to form the tight EBs. To direct the ES cells differentiation to neuronal lineage, EBs are cultured with the addition of 500 nM retinoic acid (2005820, Millipore) for four more days (4+ condition). Finally, EB formation medium (SCM018, Millipore) with 5 μg/ml laminin (Chemicon CC095, Millipore) is utilized for an additional 8 days to facilitate the expansion of neuronal cells (8− condition). Since the whole differentiation process takes place on an unconfined channel, dead volume within the developed device is minimized for efficient medium exchange. As a result, the neurogenesis of ES cells can be more efficient and accomplished. For comparison, ES cell differentiation is also performed using the same protocol for neurogenesis in Petri dishes. To further demonstrate the device capability, the EB size-dependent neurogenesis is also performed in the experiments. The EBs formed using aliquot chambers with three different dimensions (width × length: $150 \times 150\,\mu m^2$, $300 \times 300\,\mu m^2$, and $450 \times 450\,\mu m^2$, height: 250 μm) on the same device are differentiated according to the aforementioned neurogenesis protocol.

In order to observe the neurogenesis of ES cells, fluorescence immunostaining of βIII-tubulin, which has been used extensively to label newly generated neurons, is performed in the experiments.[29,30] The cells are fixed in 4% paraformaldehyde (158127, Sigma-Aldrich) in D-PBS (Gibco 14190, Invitrogen) for 30 min, and then permeablized/blocked in fresh permeable-blocking solution composed of 5% normal donkey serum (017-000-001, Jackson ImmunoResearch, West Grove, PA), 0.3% Triton X-100 (T9284, Sigma-Aldrich) in 1X D-PBS for 2 h at room temperature. Then, cells are incubated with mouse anti-βIII-tubulin (1:500) antibody (Chemicon MAB1637, Millipore) for overnight at 4 °C, washed three times, and incubated with Cy3-labeled donkey anti-mouse IgG (1:500) (Chemicon AP192C, Millipore) for 2 h in the dark. In addition, nuclei counterstaining is performed by incubating cells with 0.1 μg/ml

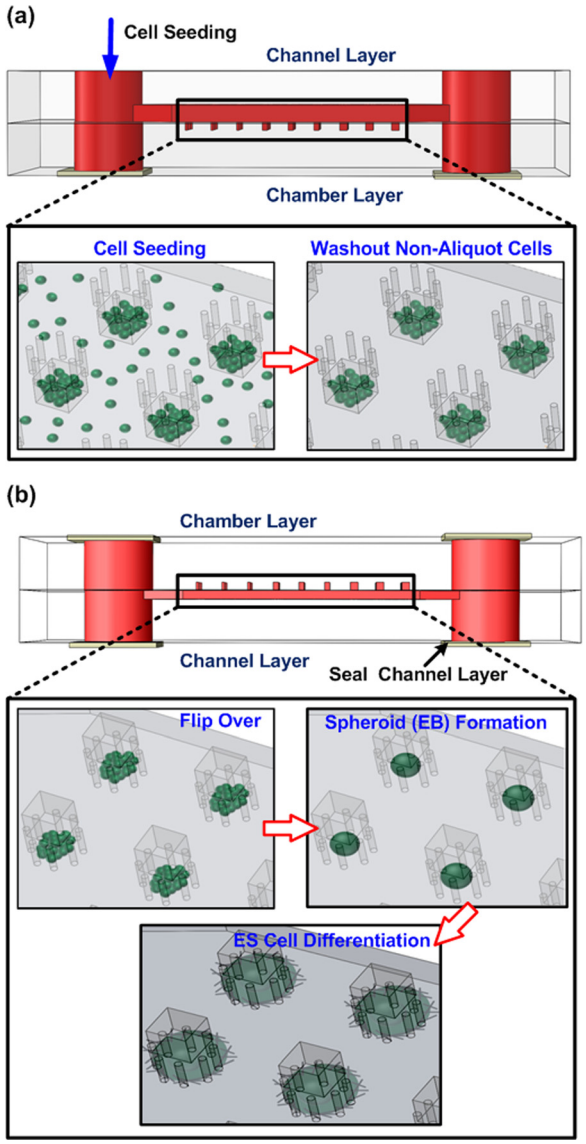

FIG. 2. Operation procedure of the flip channel device. (a) Cell aliquot process in the device. First, ES cells are introduced into the channel layer, and the non-aliquot cells are then washed out. (b) Device is flipped over for EB formation and differentiation process within the device. The loosely aggregated cells fall down to the channel layer. After 16 h of culture, the aliquot ES cells aggregate together and form EBs. The differentiation medium is then introduced into the device for ES differentiation studies.

DAPI (D9564, Sigma-Aldrich) in 1X D-PBS solution for 5 min at room temperature, followed by washing cells three times (5 min each) with 1X D-PBS.

III. RESULTS AND DISCUSSION

A. EB formation

Fig. 3(a) shows the bright field microscopic images recorded by an inverted microscope (DM-IL LED, Lecica Microsystems, Wetzlar, Germany) during the EB formation process. The images show that a specific number of cells are collected into each chamber according to its dimensions, and non-aliquot cells are washed out afterwards. The device is then flipped after 15 min to prevent cell adhesion to chambers walls due to the prolong contact and degradation of the BSA coating. The loosely packed cells then floated out from the chamber and trapped by the micro pillars. After 16-h culture,

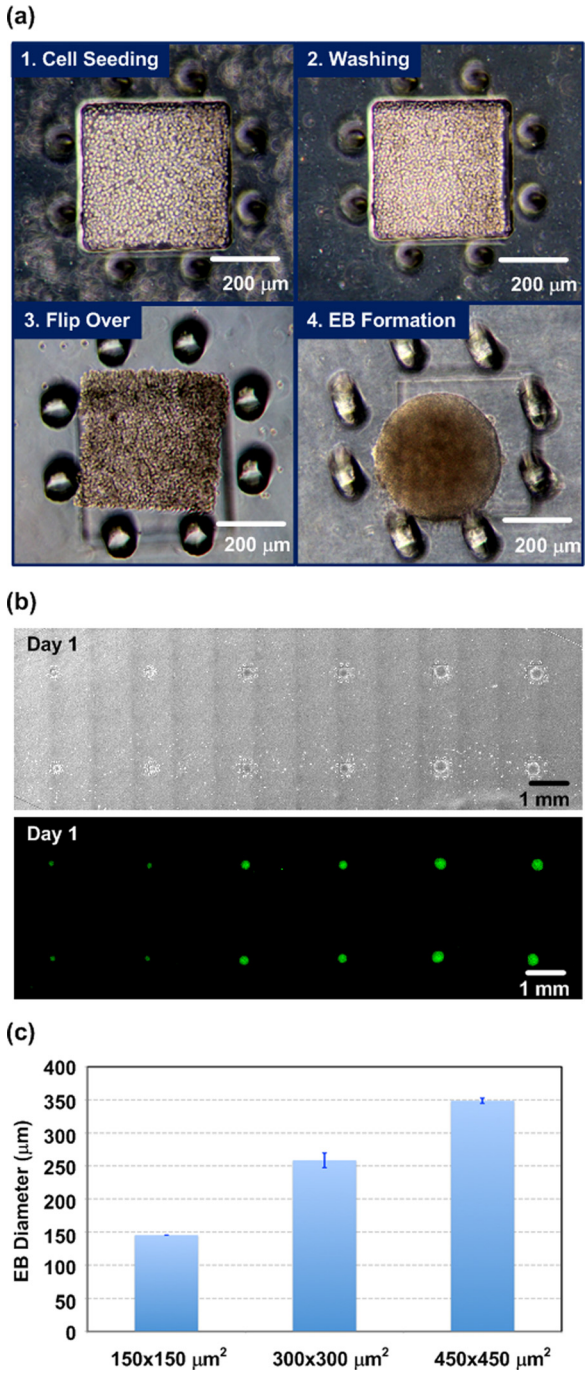

FIG. 3. (a) Time-lapse images of EB formation within the device during the operation. (b) Bright field phase and fluorescence images of EBs (Oct-GFP) formed in the developed device with different chamber dimensions. (c) Comparison of size variation of EBs formed in the device with different chamber dimensions. Data are expressed in mean ± standard deviation (n = 4).

the cells are tightly packed and form spheroids due to strong cell-cell interaction. As can be seen in the figure, EB with excellent integrity can be formed using the flip channel architecture.

Furthermore, Fig. 3(b) demonstrates the bright field phase and fluorescence microscopic images of the EBs with different sizes formed within the device after 16-h static culture after cell seeding. The green fluorescence of EBs (Oct4-GFP) suggests that the stemness of the cells is well maintained through the EB formation. In the designed device, the size of EBs can be varied by designing the dimensions of the cell aliquot chambers. The diameters of EBs are estimated by analyzing the

fluorescence images of Oct4-GFP EBs by an imaging processing program, ImageJ (Ver. 1.46r, National Institute of Health (NIH), Bethesda, MD). Figure 3(c) shows the diameters of EBs formed in the chambers with different dimensions. The results show that the average EB diameters are 145.5, 258.9, and 348.6 μm for the chambers with widths of 150, 300, and 450 μm, respectively. The shape of the formed EBs is spherical and has similar dimensions in x, y, and z directions. The variations of the diameters of EBs formed in the same dimension chambers are less than 12 μm, and the coefficients of variation (CVs) (standard deviation/mean) are less than 2.2%. In contrast, the CV of EBs formed in the Petri dish is larger than 58%.[26] The significantly lower CVs achieved using the device show that the diameters of EBs can be well controlled by simply varying the chamber dimensions.

B. EB differentiation

Figure 4(a) shows the schematic of the aforementioned EB neurogenesis procedure exploited in this paper, and Fig. 4(b) shows the bright field phase and fluorescence images of

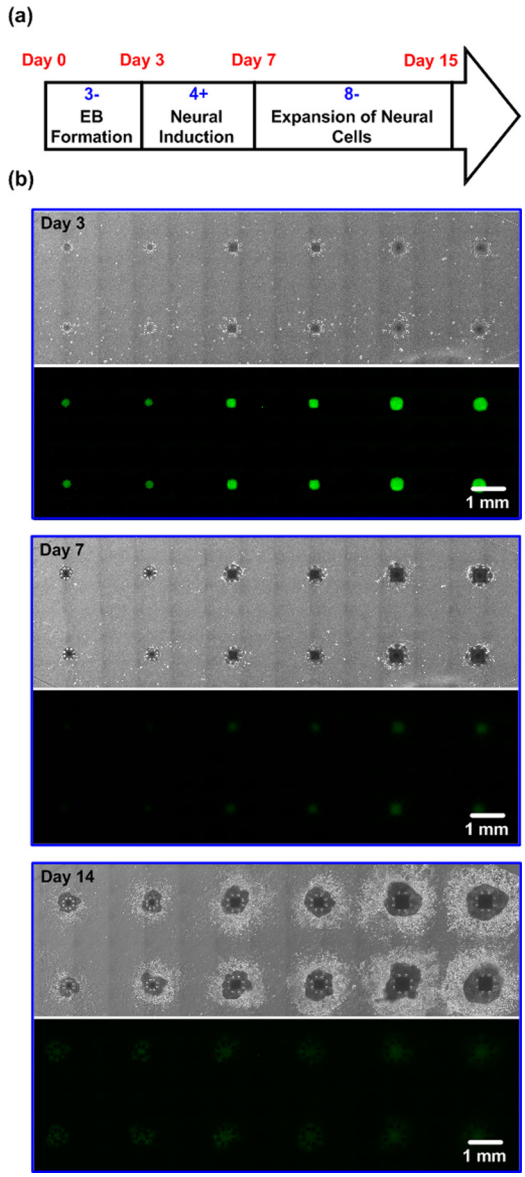

FIG. 4. (a) Schematic of EB neurogenesis protocol. (b) Bright field phase and fluorescence images of EB (Oct4-GFP) neurogenesis process within the device in different days.

an entire microfluidic device at days 3, 7, and 14 during the neurogenesis experiments. As can be seen in the images, the ES cells aggregated and formed EBs during the first three days (3−), and the sizes of EBs are slightly increased. Furthermore, the bright green fluorescence signal (oct4-GFP) suggests that the stemness of ES cells is well maintained when cultured in the microfluidic device in the format of EBs. After introducing the medium for neural induction (4+), the EBs start to attach onto the surface of the channel layer. The dimmed green fluorescence signals show that the most ES cells have been differentiated and lost their stemness. After further expansion (8−), the neuron cells grew on the flat surface of the channel layer. The image shows that the large EBs formed using $450 \times 450\,\mu m^2$ chamber have the largest outgrowth areas of neuron cells.

To further analyze the neurogenesis results, Fig. 5 shows combined fluorescence images (Red: βIII-tubulin, Green: Oct4-GFP, Blue: DAPI) of the ES cells after the entire 15-day (3−/4+/8− conditions) neurogenesis process imaged by a broadband confocal microscope (TCS SP5, Leica Microsystems). Figure 5(a) shows a fluorescence image at the neighboring area closed to the EB formation site. Some cells still show green fluorescence (Oct4-GFP), which indicates their undifferentiated states. Away from the EB formation site, more cells show red fluorescence (βIII-tubulin), which suggesting cells are differentiated to neuron cells. Figure 5(b) shows a fluorescence image at the area further away from the EB formation site in the flip channel device where ES-differentiated neuron cells have ample spaces for the outgrowth. Figures 5(c) and 5(d) show combined fluorescence images of the ES cells after the same neurogenesis process performed on Petri dishes at the area close to and away from ES colonies. Comparing the ES-differentiated cells within the device and the Petri dish, the fluorescence images show similar cell morphologies and βIII-tubulin expression. The experimental results suggest that the flat and unconfined surface makes the device developed in this research an excellent tool for the neural development study of EBs. Furthermore, the flat surface configuration makes the following cellular observation and analysis, such as immunostaining and cells harvesting, straightforward.

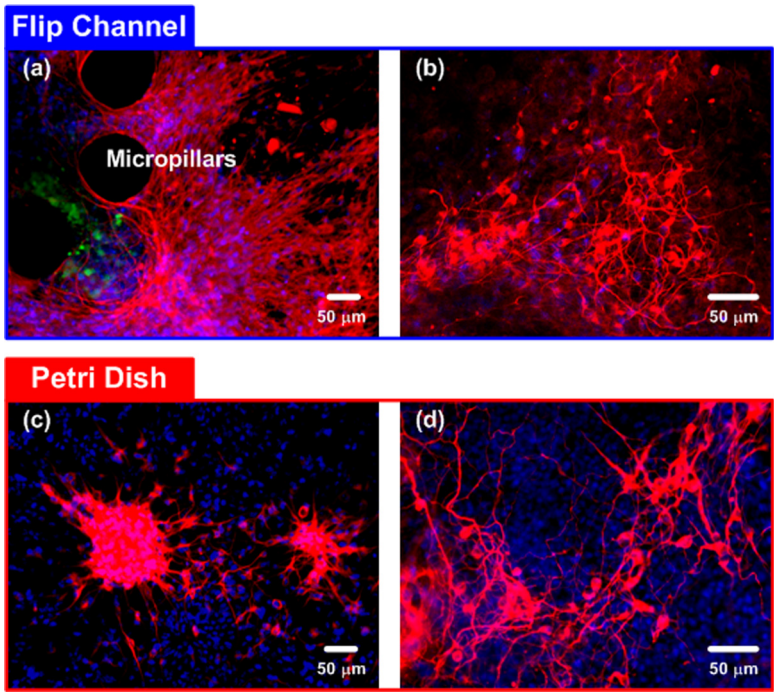

FIG. 5. Fluorescence images of Oct4-GFP (green) EB-derived neuronal differentiation in (a) and (b) developed flip channel device, and (c) and (d) Petri dish. The EBs are cultured and differentiated for 15 days (3−/4+/8− conditions), and stained with mouse βIII-tubulin (red) and DAPI (blue).

In addition, the device is exploited to study EB size-dependent neurogenesis due to the great EB size controllability as shown in Fig. 3(c). Figs. 6(a)–6(c) show the bright field phase and fluorescence images of the differentiated ES cells from EBs form in the aliquot chambers with dimensions of $150 \times 150\,\mu m^2$, $300 \times 300\,\mu m^2$, and $450 \times 450\,\mu m^2$ (width × length, and height is $250\,\mu m$), respectively. Fig. 5(d) further shows the quantitative results by analyzing the βIII-tubulin positive (red fluorescence) areas using ImageJ software, and statistical comparisons between the areas from different aliquot chamber dimensions are performed using unpaired Student's t-test. Comparing the ES-differentiated cells from different EB sizes, the experimental results show that the EB with larger diameters promotes the neurogenesis by showing more βIII-tubulin positive areas. The βIII-tubulin positive areas from EBs from the three aliquot

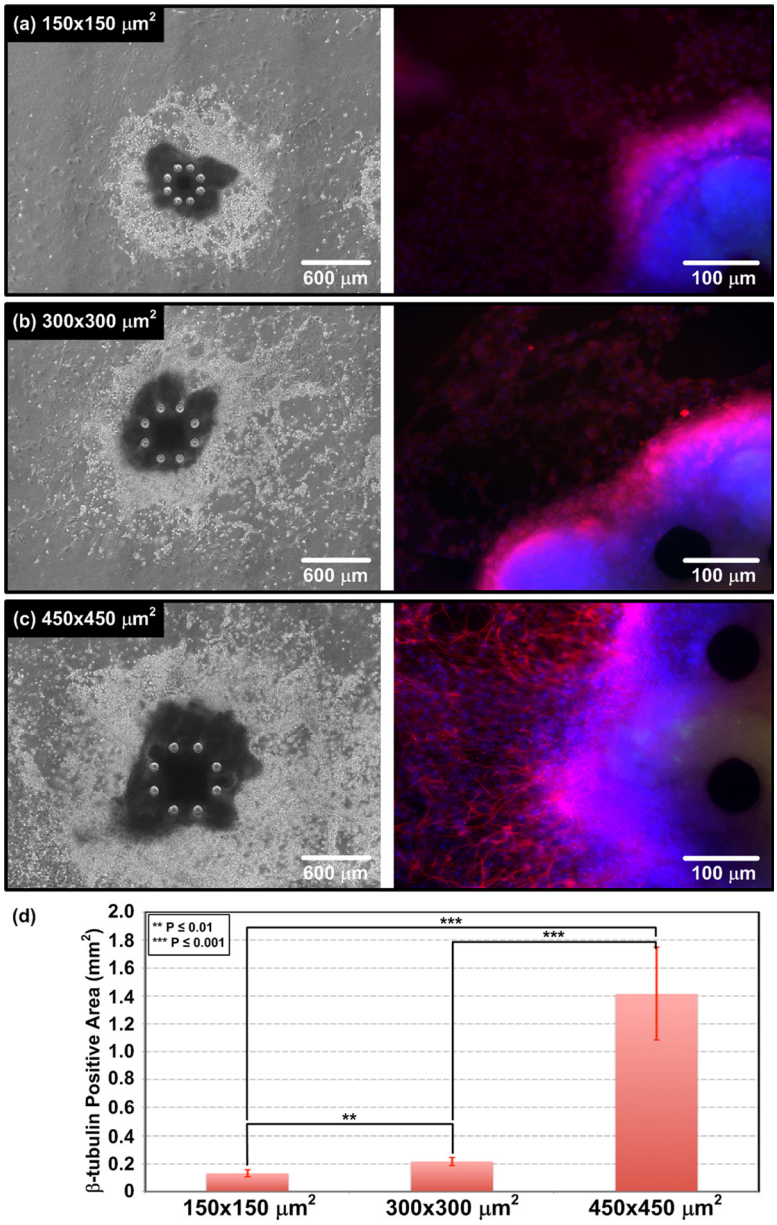

FIG. 6. (a) Bright field phase and fluorescence images of neurogenesis from EBs located in different chamber dimensions within the same device after 15-day differentiation. The cells are stained with mouse βIII-tubulin (red) and DAPI (blue). (b) Comparison of the βIII-tubulin positive areas after 15-day differentiation from EBs formed in the chambers with different dimensions. Data are expressed as the mean ± standard deviation (n = 4).

chambers are statistically different from each other. It is noticed that when the diameter of EB is about 350 μm (formed in $450 \times 450\,\mu m^2$ aliquot chambers), the βIII-tubulin positive area increase rapidly (approximately 7 times) comparing to the area from the EB with diameter of about 260 μm (formed in $300 \times 300\,\mu m^2$ aliquot chambers). The results suggest that the EB size is critical and needs to be large enough for efficient neurogenesis, which agrees with existing studies.[9] As a result, it is essential to control the EB size when conducting ES cell differentiation studies, and the experimental results demonstrate the great functionality provided by the developed flip channel device.

IV. CONCLUSIONS

In this paper, Flip channel—a simple double-layered PDMS microfluidic device capable of forming uniform-sized EB and further proceeding to the following differentiation study in the same device is developed. Despite a number of chips have been developed to form uniform-sized EBs at the designed position, however, the EBs need to be cultivated from the devices and transferred to other substrates for further differentiation experiments. Consequently, it is challenging to simultaneously monitor the same EBs before and after the differentiation experiments. In our device, the size of the EBs can be controlled by varying the geometries of cell aliquot chambers. Furthermore, the integrity and stemness of EBs are well maintained in the device due to the static EB formation process without additional mechanical stimulation. By easily flipping over the device, the differentiation of EBs can be taken place on a flat surface without mechanical confinements, and the entire process can be continuously observed for better biology studies. In the experiments, the formation of uniformed-sized EBs (ES-D3) and their differentiation to neural cells are demonstrated. The results show that the differentiated neural cells within the device have similar morphologies and βIII-tubulin expression to those in a Petri dish. In addition, the EB size-dependent ES cell differentiation can also be efficiently investigated within a single device using the developed flip channel device. The developed device allows the EBs attached to the designed position in a flat PDMS channel and differentiates in the same device without sophisticated sample handling. These breakthroughs enable many following investigations on stem cells under controlled microenvironments, such as the role of cell co-culture and mechanical cues in the fate decision of stem cells.

ACKNOWLEDGMENTS

The authors would like to thank Ms. Yung-Ju Cheng and Mr. Wei-Hao Liao for their help in the experiments. This paper is based on work supported by the National Health Research Institutes (NHRI) in Taiwan under a Career Development Grant (CDG) (Grant No. EX103-10021EC), the Taiwan Ministry of Science and Technology (MOST 101-2628-E-001-002-MY3, 103-2221-E-001-001-MY2, and 104-2221-E-001-015-MY3), and the Academia Sinica Research Program on Nanoscience and Nanotechnology.

[1]S. M. Dang, S. Gerecht-Nir, J. Chen, J. Itskovitz-Eldor, and P. W. Zandstra, "Controlled, scalable embryonic stem cell differentiation culture," Stem Cells **22**, 275–282 (2004).
[2]H. Kurosawa, "Methods for inducing embryoid body formation: In vitro differentiation system of embryonic stem cells," J. Biosci. Bioeng. **103**, 389–398 (2007).
[3]Y. Torisawa, B.-H. Chueh, D. Huh, P. Ramamurthy, T. M. Roth, K. F. Barald, and S. Takayama, "Efficient formation of uniform-sized embryoid bodies using a compartmentalized microchannel device," Lab Chip **7**, 770–776 (2007).
[4]C. M. Cameron, W.-S. Hu, and D. S. Kaufman, "Improved development of human embryonic stem cell-derived embryoid bodies by stirred vessel cultivation," Biotechnol. Bioeng. **94**, 938–948 (2006).
[5]B. Bhattacharya, S. Puri, and R. K. Puri, "A review of gene expression profiling of human embryonic stem cell lines and their differentiated progeny," Curr. Stem Cell Res. Ther. **4**, 98–106 (2009).
[6]V. F. M. Segers and R. T. Lee, "Stem-cell therapy for cardiac disease," Nature **451**, 937–942 (2008).
[7]B. E. Reubinoff, M. F. Pera, C. Y. Fong, A. Trounson, and A. Bongso, "Embryonic stem cell lines from human blastocysts: Somatic differentiation in vitro," Nat. Biotechnol. **18**, 399–404 (2000).
[8]Y.-S. Hwang, B. G. Chung, D. Ortmann, N. Hattori, H.-C. Moeller, and A. Khademhosseini, "Microwell-mediated control of embryoid body size regulates embryonic stem cell fate via differential expression of WNT5a and WNT11," Proc. Natl. Acad. Sci. U. S. A. **106**, 16978–16983 (2009).
[9]Y. Y. Choi, B. G. Chung, D. H. Lee, A. Khademhosseini, J.-H. Kim, and S.-H. Lee, "Controlled-size embryoid body formation in concave microwell arrays," Biomaterials **31**, 4296–4303 (2010).

[10]D. ten Berge, W. Koole, C. Fuerer, M. Fish, E. Eroglu, and R. Nusse, "Wnt signaling mediates self-organization and axis formation in embryoid bodies," Cell Stem Cell **3**, 508–518 (2008).
[11]D. ten Berge, D. Kurek, T. Blauwkamp, W. Koole, A. Maas, E. Eroglu, R. K. Siu, and R. Nusse, "Embryonic stem cells require Wnt proteins to prevent differentiation to epiblast stem cells," Nature Cell Biol. **13**, 1070–1075 (2011).
[12]J. Pihl, J. Sinclair, E. Sahlin, M. Karlsson, F. Petterson, J. Olofsson, and O. Orwar, "Microfluidic gradient-generating device for pharmacological profiling," Anal. Chem. **77**, 3897–3903 (2005).
[13]D. Huh, H. Fujioka, Y.-C. Tung, N. Futai, R. Paine, J. B. Grotberg, and S. Takayama, "Acoustically detectable cellular-level lung injury induced by fluid mechanical stresses in microfluidic airway systems," Proc. Natl. Acad. Sci. U. S. A. **104**, 18886–18891 (2007).
[14]A. Shamloo, N. Ma, M.-M. Poo, L. L. Sohn, and S. C. Heilshorn, "Endothelial cell polarization and chemotaxis in a microfluidic device," Lab Chip **8**, 1292–1299 (2008).
[15]Y. Kamotani, T. Bersano-Begey, N. Kato, Y.-C. Tung, D. Huh, J. W. Song, and S. Takayama, "Individually programmable cell stretching microwell arrays actuated by a Braille display," Biomaterials **29**, 2646–2655 (2008).
[16]S. Kim, H. J. Kim, and N. L. Jeon, "Biological applications of microfluidic gradient devices," Integr. Biol. **2**, 584–603 (2010).
[17]M.-C. Liu, H.-C. Shih, J.-G. Wu, T.-W. Weng, C.-Y. Wu, J.-C. Lu, and Y.-C. Tung, "Electrofluidic pressure sensor embedded microfluidic device: A study of endothelial cells under hydrostatic pressure and shear stress combinations," Lab Chip **13**, 1743–1753 (2013).
[18]L. L. Bischel, E. W. K. Young, B. R. Mader, and D. J. Beebe, "Tubeless microfluidic angiogenesis assay with three-dimensional endothelial-lined microvessels," Biomaterials **34**, 1471–1477 (2013).
[19]O. F. Khan and M. V. Sefton, "Perfusion and characterization of an endothelial cell-seeded modular tissue engineered construct formed in a microfluidic remodeling chamber," Biomaterials **31**, 8254–8261 (2010).
[20]C.-W. Chang, Y.-J. Cheng, M. Tu, Y.-H. Chen, C.-C. Peng, W.-H. Liao, and Y.-C. Tung, "A polydimethylsiloxane-polycarbonate hybrid microfluidic device capable of generating perpendicular chemical and oxygen gradients for cell culture studies," Lab Chip **14**, 3762–3772 (2014).
[21]Y. Torisawa, B. Mosadegh, G. D. Luker, M. Morell, K. S. O'Shea, and S. Takayama, "Microfluidic hydrodynamic cellular patterning for systematic formation of co-culture spheroids," Integr. Biol. **1**, 649–654 (2009).
[22]E. Ghafar-Zadeh, J. R. Waldeisen, and L. P. Lee, "Engineered approaches to the stem cell microenvironment for cardiac tissue regeneration," Lab Chip **11**, 3031–3048 (2011).
[23]E. Kang, Y. Y. Choi, Y. Jun, B. G. Chung, and S.-H. Lee, "Development of a multi-layer microfluidic array chip to culture and replate uniform-sized embryoid bodies without manual cell retrieval," Lab Chip **10**, 2651–2654 (2010).
[24]Y.-C. Tung, A. Y. Hsiao, S. G. Allen, Y. Torisawa, M. Ho, and S. Takayama, "High-throughput 3D spheroid culture and drug testing using a 384 hanging drop array," Analyst **136**, 473–478 (2011).
[25]G. S. Jeong, Y. Jun, J. H. Song, S. H. Shin, and S.-H. Lee, "Meniscus induced self organization of multiple deep concave wells in a microchannel for embryoid bodies generation," Lab Chip **12**, 159–166 (2012).
[26]B. Patra, Y.-H. Chen, C.-C. Peng, S.-C. Lin, C.-H. Lee, and Y.-C. Tung, "A microfluidic device for uniform-sized cell spheroids formation, culture, harvesting and flow cytometry analysis," Biomicrofluidics **7**, 054114 (2013).
[27]W. G. Lee, D. Ortmann, M. J. Hancock, H. Bae, and A. Khademhosseini, "A hollow sphere soft lithography approach for long-term hanging drop methods," Tissue Eng., Part C **16**, 249–259 (2010).
[28]J.-C. Lu, W.-H. Liao, and Y.-C. Tung, "Magnet-assisted device-level alignment for fabrication of membrane-sandwiched polydimethylsiloxane (PDMS) microfluidic devices," J. Micromech. Microeng. **22**, 75006–75013 (2012).
[29]C. N. Svendsen, A. Bhattacharyya, and Y. T. Tai, "Neurons from stem cells: Preventing an identity crisis," Nat. Rev. Neurosci. **2**, 831–834 (2001).
[30]C. D. Katsetos, M. M. Herman, and S. J. Mörk, "Class III beta-tubulin in human development and cancer," Cell Motil. Cytoskeleton **55**, 77–96 (2003).